Essential roles of Xenopus TRF2 in telomere end protection and replication.

AUTHOR(S):

Muraki, Keiko; Nabetani, Akira; Nishiyama, Atsuya; Ishikawa, Fuyuki

Essential Roles of *Xenopus* TRF2 in Telomere End Protection and Replication

Keiko Muraki[1], Akira Nabetani[1], Atsuya Nishiyama[1,2], and Fuyuki Ishikawa[1,*]

[1]Laboratory of Cell Cycle Regulation, Department of Gene Mechanisms,
Graduate School of Biostudies, Kyoto University,
Yoshida-Konoe-cho, Sakyo-ku,
Kyoto 606-8501, Japan

Running title: *Xenopus* TRF2 and telomeres

Total length of the manuscript: 43,768 characters including spaces

*Correspondence to Fuyuki Ishikawa
(fishikaw@lif.kyoto-u.ac.jp, and FAX: 81-75-753-4197)

[1] Laboratory of Cell Cycle Regulation, Department of Gene Mechanisms,
Graduate School of Biostudies, Kyoto University,
Yoshida-Konoe-cho, Sakyo-ku, Kyoto 606-8501, Japan

[2] Present address: Institute of Human Genetics, CNRS, 34396 Montpellier, France

Abstract

TRF1 and TRF2 are double-stranded (ds) telomere DNA-binding proteins and the core members of shelterin, a complex that provides the structural and functional basis of telomere functions. We have reported that unlike mammalian TRF1 that constitutively binds to chromatin, *Xenopus* TRF1 (xTRF1) associates with mitotic chromatin but dissociates from interphase chromatin reconstituted in *Xenopus* egg extracts. This finding raised the possibility that xTRF1 and *Xenopus* TRF2 (xTRF2) contribute to telomere functions in a manner different from mammalian TRF1 and TRF2. Here we focused on the role of xTRF2. We prepared chromatin reconstituted in egg extracts immunodepleted for xTRF2. Compared to mock-depleted nuclei, DNA damage response at telomeres was activated and bulk DNAs were poorly replicated in xTRF2-depleted nuclei. The replication defect was rescued by inactivating ATR through the addition of anti-ATR neutralizing antibody, suggesting that ATR plays a role in the defect. Interestingly, the bulk DNA replication defect, but not the DNA damage response at telomeres, was rescued by supplementing the xTRF2-depleted extracts with recombinant xTRF2 (rTRF2). We propose that xTRF2 is required for both efficient replication of bulk DNA and protection from the activation of the DNA damage checkpoints pathway, and that those two functions are mechanistically separable.

Introduction

The telomere is a specialized nucleoprotein complex at the chromosomal ends and essential for genomic stability. Telomere DNA consists of tandem repeats of ds DNA and each strand is guanine- or cytosine-rich (called G- or C-strand, respectively). The 3'-end of the G-strand forms a single-stranded (ss) extension termed the G-tail. A conserved protein complex called shelterin provides the structural and functional basis of telomere chromatin (Miyoshi *et al.* 2008; Palm & de Lange 2008). Mammalian shelterin consists of six component proteins, TRF1, TRF2, Rap1, TIN2, TPP1, and POT1. Among them, TRF1 and TRF2 directly bind to ds telomere DNA repeats (TTAGGG)/(CCCTAA) as homodimers and POT1 binds to ss G-tail.

The two major tasks of telomeres are to protect DNA ends from degradation and fusion, and to facilitate replication of DNA ends via the conventional semi-conservative replication and telomerase. Defects in telomere protection frequently induce chromosomal end-to-end fusions. Deprotected telomeres leading to the fusion are typically observed when mammalian TRF2 is inhibited by the over-expression of a dominant-negative form of TRF2 (van Steensel *et al.* 1998), indicating that TRF2 is responsible for the protection of telomeres in mammalian cells. When TRF2 is inhibited, damage-response markers are accumulated at telomeres, a cytological observation called telomere dysfunction-induced foci (TIFs) (Takai *et al.* 2003). The markers include phosphorylated histone H2AX (γ-H2AX), phosphorylated Rad17 (p-Rad17), and the Mre11-Rad50-Nbs1 (MRN) complex. Because those markers are typically detected at DNA double-strand break (DSB) sites, it is suggested that TIF formation indicates the deprotection of telomere end. Another task of telomeres is to facilitate

DNA replication at telomeres. Because telomere DNAs are repetitive sequences that potentially form higher-ordered DNA structures, it has been long expected that telomere DNAs pose difficulties in conventional DNA replication machineries. Indeed, it is now known that mammalian telomeres are one of the fragile sites, specific regions in the genome where the replication reaction tends to be stalled (Sfeir *et al.* 2009). Those regions potentially form DSBs by processing unreplicated ss DNA, and chromatid/chromosome breaks in M phase (Durkin & Glover 2007). It has been reported that TRF1 is required for the proficient replication of telomere DNAs in mammalian cells (Sfeir *et al.* 2009).

Those studies indicate that shelterin components are responsible for the different roles of telomeres. Specifically, TRF1 and TRF2 are required for telomere DNA replication and telomere protection, respectively. Functionally insufficient telomeres activate DNA damage checkpoints, being recognized by two DNA-damage-sensor protein kinases, ATM and ATR, members of the phosphatidylinositol 3-kinase related kinase (PIKK) family. In mammals, ATM and ATR are activated by different sets of DNA damages: ATM responds to DSBs, whereas ATR is activated by replication fork stalling and ss DNAs (Abraham 2001). Once activated, they phosphorylate numerous downstream substrates including Cds1/Chk2 and Chk1. The inactivation of TRF2 leads to the recognition of telomere DNA ends as DSBs, and this leads to the activation of ATM-dependent DNA damage checkpoint pathways (Karlseder *et al.* 1999). TRF1 deletions, meanwhile, lead to the activation of ATR (McNees *et al.* 2010; Sfeir *et al.* 2009).

Xenopus egg extracts are a rich source of nuclear proteins and recapitulate cell-cycle-related events *in vitro*. When demembraned *Xenopus* sperm chromatin is

incubated with interphase *Xenopus* egg extracts, the chromatin becomes decondensed, forms interphase nuclei demarcated by the nuclear membrane, and undergoes semi-conservative DNA replication. We have shown that shelterin components are conserved in *Xenopus* and the egg extracts provide a good model system to analyze telomere functions during the cell cycle. Specifically, we found that *Xenopus* TRF1 (xTRF1) associates with mitotic chromatin but dissociates from the interphase chromatin upon the cell cycle's entry to interphase in a replication-independent manner. In contrast, *Xenopus* TRF2 (xTRF2) constitutively associates with chromatin throughout the cell cycle (Nishiyama *et al.* 2006). Given that mammalian TRF1 is required for the efficient DNA replication at telomeres in S phase, our observations raise the question of whether or not xTRF2, rather than xTRF1, facilitates DNA replication at telomeres in the *Xenopus* egg extract system. In this study, we focused on the role of xTRF2 in the end protection and replication of telomeres in the *Xenopus* egg extracts.

Results

xTRF2 is a homologue of mammalian TRF2 and localizes at telomeres

TRF1 and TRF2 show similar domain organizations: They share TRFH (telomeric repeat binding factor homology) and Myb domains at the C-termini. The N-terminal regions of mammalian TRF1 and TRF2 are characterized by the presence of acidic and basic regions, respectively. In contrast, xTRF1 and xTRF2 do not possess significantly acidic or basic regions at their N-termini (Fig. 1A). The predicted xTRF amino acid sequences were not mistakenly deduced from 5'-truncated cDNAs because numerous xTRF1 EST (expressed sequence tag) sequences in the database had predicted an open-reading frame that has an in-frame stop codon upstream (-39 nt in xTRF1). Similarly, an in-frame stop codon upstream was found in *Xenopus tropicalis* TRF2 (-147 nt), although not in *Xenopus laevis* TRF2 cDNA.

Several lines of evidence suggest that xTRF1 and xTRF2 are homologues of mammalian TRF1 and TRF2, respectively. We first compared the amino acid sequences of the TRFH and Myb domains, and the linker region connecting the two domains between xTRF1 or xTRF2 and human TRF1 (hTRF1) or human TRF2 (hTRF2). Higher sequence identities and similarities were observed between TRF1 proteins and between TRF2 proteins derived from *Xenopus laevis* and human than between xTRF1 and xTRF2 (Nishiyama *et al.* 2006). It is known that TIN2 binds to both TRF1 and TRF2 in mammalian cells. Five of the seven amino acid residues of hTRF1 important for the interaction with human TIN2 (Chen *et al.* 2008) are conserved in xTRF1 but not in xTRF2. Similarly, the region in hTRF2 that is required and sufficient for the interaction with hTIN2 (Chen *et al.* 2008) shows higher homology with the corresponding region in

xTRF2 than with that in xTRF1 (Fig. 1C). Mouse TRF2 (mTRF2) interacts with mouse Rap1 (mRap1) through a conserved region between human and mouse (Sfeir *et al.* 2010). This region shows higher homology with the corresponding region in xTRF2 than with that in xTRF1 (Fig. 1C). hTRF2 F292, which corresponds to mTRF2 F290, one of the crucial amino acids for the interaction with mRap1, is conserved in xTRF2 (xTRF2 F267) but not in xTRF1. Finally, hTRF2 regions required for the interaction with human Apollo (hApollo) are conserved in xTRF2, but not in xTRF1 (Fig. 1B). From these results, we conclude that xTRF1 and xTRF2 are homologues of mammalian TRF1 and TRF2, respectively.

xTRF2 specifically binds to ds telomere repeat DNA and is associated with reconstituted chromatin in both mitotic and interphase extracts (Nishiyama *et al.* 2006). We investigated whether endogenous xTRF2 is localized at the telomeres or not. We incubated *Xenopus* sperm chromatin for 90 min with interphase *Xenopus* egg extracts and then simultaneously examined the localizations of xTRF2 and telomere DNAs by indirect immunofluorescence experiments using anti-xTRF2 antibody and fluorescence *in situ* hybridization (FISH) experiments employing $(CCCTAA)_3$ PNA (peptide-nucleic acid) as a probe, respectively (Fig. 2A). Focal signals of xTRF2 and telomere DNA were observed and a stack of images were recorded along the z-axis. The images were processed by deconvolution to highlight the focal signals. We observed 27.1±8.7 xTRF2 foci and 24.7±7.0 telomere DNA foci in one nucleus (n=60 nuclei). 88.1±8.3% of the xTRF2 foci were merged with the telomere DNA foci, and 95.8±5.6% of the telomere DNA foci were merged with the xTRF2 foci. These results indicate that endogenous xTRF2 is specifically localized at telomeres in chromatin reconstituted in interphase egg extracts.

xTRF2 is required for telomere recruitment of xPOT1

To investigate the function of xTRF2, we prepared interphase egg extracts immunodepleted for xTRF2 using anti-xTRF2 antibody (ΔTRF2 extracts) and mock-depleted extracts using normal rabbit IgG (Δmock extracts) as a control. Sperm chromatin incubated with these extracts for 90 min was isolated and analyzed by immunofluorescence and immunoblotting. We did not observe colocalization of xTRF2 immunofluorescence signals and telomere FISH signals in chromatin formed in ΔTRF2 extracts (Fig. 2A, ΔTRF2 nuclei). Chromatin-bound xTRF2 was detected in chromatin reconstituted in Δmock extracts (Δmock nuclei), but not in ΔTRF2 nuclei (Fig. 2B). Interestingly, chromatin-bound *Xenopus* POT1 (xPOT1) was detected in Δmock nuclei but not in ΔTRF2 nuclei (Fig. 2B). When ΔTRF2 extracts were supplemented with rTRF2 prior to incubation with sperm chromatin, rTRF2 localized at telomeres (Fig. 2A, rTRF2+ΔTRF2 nuclei) and xTRF2 and xPOT1 were detected in the chromatin fraction (Fig. 2B). These results suggest that xPOT1 associates with chromatin in an xTRF2-dependent manner. Geminin is an inhibitor of replication-initiating factor Cdt1. The addition of recombinant geminin protein to the extracts inhibited the replication both in ΔTRF2 and Δmock extracts, as expected (Fig. S1A in Supporting Information). xTRF2 and xPOT1 bound to chromatin in the presence of geminin, suggesting that DNA replication is not required for the recruitment of xTRF2 and xPOT1 to chromatin (Fig. 2C). We have previously found that xTRF1 dissociates from interphase chromatin in egg extracts (Nishiyama *et al.* 2006). Therefore, we assume that most, if not all, shelterin complex components are removed from telomere chromatin formed in ΔTRF2 extracts.

To test the function of xTRF2 on the behavior of xTRF1, we examined the association of xTRF1 with chromatin in both ΔTRF2 and Δmock extracts. We found that xTRF1 bound to mitotic chromatin formed in ΔTRF2 and Δmock mitotic CSF (cytostatic-factor-arrested) extracts (see Experimental Procedure) and dissociated from the chromatin upon entry into interphase by the addition of Ca^{2+} to the ΔTRF2 and Δmock mitotic CSF extracts. This suggests that xTRF2 is dispensable for the cell-cycle-dependent chromatin association of xTRF1 (Fig. S1B in Supporting Information).

Depletion of xTRF2 induces TIFs

TRF2-defective mammalian cells show deprotected telomeres, as revealed by the presence of TIFs (Takai *et al.* 2003). To investigate whether telomeres of ΔTRF2 nuclei form TIFs, we measured the frequency of γ-H2AX-positive telomere FISH signals (TIFs) among the total FISH signals in one nucleus (Figs. 3A, B). In ΔTRF2 and Δmock nuclei, 64.3±4.0% and 0.3±0.3% of the telomeres were γ-H2AX-positive, respectively (n=40 nuclei), indicating the induction of DNA damage response at the telomeres in ΔTRF2 nuclei. The increase of TIFs in ΔTRF2 nuclei was not suppressed by the addition of rTRF2 to the extracts. As shown in Fig. 3B, the TIF frequency in ΔTRF2+rTRF2 nuclei (88.7±2.2%, n=40 nuclei) was significantly larger than that in Δmock+rTRF2 nuclei (0.1±0.1%, n=40 nuclei). Interestingly, the increase of TIFs in ΔTRF2 nuclei was not affected by the inhibition of DNA replication by geminin. TIF frequency in ΔTRF2+geminin nuclei (66.7±3.0%, n=56 nuclei) was significantly increased compared to that in Δmock+geminin nuclei (0.5±0.3%, n=56 nuclei) (Fig. 3C).

We also observed the localization of other damage-response markers, p-Rad17 and *Xenopus* NBS1 (xNBS1), and found that anti-p-Rad17 antibody stained telomeres in ΔTRF2 nuclei but not in Δmock nuclei (Fig. S2 in Supporting Information). The accumulation of p-Rad17 at telomeres was not inhibited by supplying rTRF2 (+rTRF2; Figs. S2A, B in Supporting Information) or replication inhibition by geminin (+Gem; Fig. S2C in Supporting Information). Furthermore, xNBS1 foci were observed at telomeres in ΔTRF2 nuclei, but not in Δmock nuclei (Fig. S3). The accumulation of xNBS1 at telomeres was not suppressed by rTRF2 (+rTRF2; Figs. S3A, B in Supporting Information) or the replication inhibition by geminin (+Gem; Fig. S3C in Supporting Information). xNBS1 was detected at telomeres even when five-fold larger amount of rTRF2 than that used in Fig. S3 was added to ΔTRF2 nuclei, suggesting that the persistent xNBS1 was not caused by insufficient supply of rTRF2 to the extracts (Fig. S4). These results indicate that TIFs are formed in ΔTRF2 nuclei in a replication-independent manner.

ATM is a member of the PIKK family and is activated in DNA damage and deprotected telomeres by TRF2 inhibition in mammalian cells (Bakkenist *et al.* 2004; Lazzerini Denchi & de Lange 2007). To examine whether the ATM pathway is activated in ΔTRF2 nuclei, we analyzed whether ATM is phosphorylated or not. The phosphorylated form of ATM (p-ATM) was observed in ΔTRF2 extracts. Supplying rTRF2 (+rTRF2) or replication inhibition by geminin (+Gem) did not abolish the p-ATM signal from ΔTRF2 extracts (Fig. S5 in Supporting Information). This suggests that ATM is activated in ΔTRF2 extracts and the activation is independent of replication, as in the case of TIF formation in ΔTRF2 nuclei.

ATR but not ATM regulates bulk DNA replication in ΔTRF2 extracts

We next measured the overall replication efficiency. Sperm chromatin was incubated with interphase egg extracts in the presence of [α-^{32}P]dCTP. Samples were collected at intervals, purified DNAs were resolved by gel electrophoresis, and autoradiography of incorporated ^{32}P signals was conducted (Fig. S6A in Supporting Information). The overall replication efficiency of the whole genome was determined as described in Experimental Procedures. As shown in Fig. 4A, the replication in Δmock nuclei was almost completed at 90-min incubation. In ΔTRF2 nuclei, the replication efficiency was reduced to approximately half of that in Δmock nuclei. When ΔTRF2 extracts were supplemented with rTRF2, the replication efficiency was recovered to the control level. These results indicate that xTRF2 is required for the efficient replication of whole sperm chromatin.

As described above, DNA damage response is activated and replication is repressed in ΔTRF2 nuclei. We therefore examine whether ATM and/or ATR regulates the replication efficiency. We inhibited the ATM or ATR pathway with KU55933, an ATM-specific inhibitor, or anti-*Xenopus* ATR (anti-xATR) neutralizing antibody, respectively. Those treatments effectively inhibited the downstream pathways, as measured in terms of Cds1 and Chk1 phosphorylation levels (Figs. S6B, C in Supporting Information). We found that the inhibition of ATR rescued the low replication efficiency in ΔTRF2 extracts, whereas the inhibition of ATM did not (Figs. 4B, C). Treatment of the ΔTRF2 extracts with caffeine, an inhibitor of both ATM and ATR kinases also rescued the replication efficiency (Fig. S6D in Supporting Information). The Chk1 inhibitor, UCN-01 only partially relieved the replication inhibition in ΔTRF2 extracts (Fig. 4D). These results indicate that the activation of ATR,

not ATM, is responsible for the low replication efficiency in ΔTRF2 nuclei.

We also analyzed the replication kinetics of each of three loci in the genome, telomere, centromere and 5S RNA genes. Sperm chromatin was incubated with interphase egg extracts in the presence of bromodeoxyuridine triphosphate (BrdUTP). DNA samples were collected at intervals, sonicated and fractionated by CsCl equilibrium density gradient ultracentrifugation. The fractionated DNAs were examined by blot hybridization with specific probes (see Supplemental Experimental Procedures). As shown in Supplementary text and Fig. S7 in Supporting Information, telomere regions are replicated in earlier kinetics than the centromere or 5S RNA genes. This result suggests that the telomere is an early replicating region in *Xenopus* sperm chromatin, and raised the possibility that a defect of telomere replication in ΔTRF2 nuclei may inhibit the replication of late replicating regions.

Loss of telomere FISH signals in ΔTRF2 nuclei

We found that the number of telomere FISH signals was significantly smaller in ΔTRF2 nuclei than in Δmock nuclei; there were 10.9±0.7 FISH signals in one ΔTRF2 nucleus and 19.0±0.7 in one Δmock nucleus (n=125 nuclei, $p<0.001$, Figs. 5A, B). When ΔTRF2 extracts were supplemented with rTRF2, the number of FISH signals was recovered to the level of Δmock nuclei (21.1±0.9 foci/nucleus, n=125 nuclei). To test whether the loss of telomere FISH signal is dependent on replication in ΔTRF2 nuclei, we inhibited the replication reaction in ΔTRF2 extracts. When the extract was treated with geminin, the number of FISH signals in ΔTRF2 nuclei was not reduced (21.2±1.4 foci/nucleus, n=77 nuclei, Figs. 5C) compared to that in Δmock nuclei with or without geminin treatment, suggesting that telomeres that have undergone replication in the

absence of xTRF2 lose telomere FISH signals.

To analyze the mechanism of the loss of the telomere FISH signals, we analyzed telomere length in ΔTRF2 nuclei and found that the telomere lengths of both G strand and C strand were not altered in ΔTRF2 nuclei (Fig. 5D). The exact nature of the telomere replication defects in ΔTRF2 nuclei, which lead to the loss of telomere FISH signals, remains to be elucidated in the future.

Discussion

xTRF1 and xTRF2 are unique compared to their mammalian counterparts; they lack the N-terminal acidic and basic regions that characterize mammalian TRF1 and TRF2, respectively (Nishiyama *et al.* 2006). It was reported that chicken TRF1 and TRF2 do not possess the N-terminal acidic domain and the basic domain, respectively (De Rycker *et al.* 2003; Konrad *et al.* 1999). Meanwhile, the amino acid residues required for the interaction with TIN2 and Apollo show higher homology between TRF1s and TRF2s in chicken and humans, suggesting that the protein binding domains characterize TRF1 and TRF2 proteins among different species. xTRF1 and xTRF2 behave differently during the cell cycle: xTRF1 associates with mitotic chromatin but not with interphase chromatin in egg extracts, whereas xTRF2 associates with both mitotic and interphase chromatins. In contrast, both mammalian TRF1 and TRF2 constitutively bind to telomere chromatin. We do not know whether the cell-cycle-dependent chromatin association of xTRF1 is common to all *Xenopus* somatic cells, unique to early development or *in vitro* reconstituted chromatin. We found that chromatin-bound xPOT1 was largely lost in ΔTRF2 nuclei (Fig. 2B). As xTRF2 is the only ds telomere DNA-binding protein in interphase chromatin, it is expected that the removal of xTRF2 would lead to the collapse of the whole shelterin complex. Interestingly, xTRF1 is bound to the mitotic chromatin of ΔTRF2 nuclei (Fig. S1B in Supporting Information). This suggests that shelterin can be partially formed in the mitotic chromatin in an xTRF2-independent manner. In mammalian cells, the inactivation of TRF2 leads to the reduced association of POT1a, TPP1 and TIN2 at telomeres (Konishi & de Lange 2008;

Lazzerini Denchi & de Lange 2007; Loayza & de Lange 2003). It is unknown whether the dependence of mammalian shelterin formation on TRF2 is altered during the cell cycle.

DNA damage response in ΔTRF2 nuclei

A deficiency in telomere end protection results in damage response at telomeres, as characterized by ATM activation and the formation of TIFs (Takai *et al.* 2003). TIFs are formed in TRF2-deficient mammalian cells, indicating that TRF2 is required for the end protection at telomeres. We observed TIFs and p-ATM in ΔTRF2 nuclei (Figs. 3 and S2-5 in Supporting Information), indicating that xTRF2 is required for telomere end protection and suppression of ATM activation in the interphase nuclei. We found TIFs and p-ATM in ΔTRF2 extracts in both the absence and presence of geminin, indicating that ATM activation and DNA damage response in ΔTRF2 nuclei are replication-independent. Similarly, TIFs are formed in G0, G1 and S/G2 phases in TRF2-deficient mouse cells (Konishi & de Lange 2008). We propose that xTRF2 (and xPOT1) removal directly causes the deprotection of telomeres (Fig. 5E, pathway a). Unexpectedly, we observed that both TIF formation and the ATM activation in ΔTRF2 nuclei were not suppressed by the addition of rTRF2 to egg extracts. It is possible that the removal of both xTRF2 and xPOT1 in ΔTRF2 nuclei was too harsh to allow the re-establishment of functional shelterin by simply supplying rTRF2. Alternatively, the removal of xTRF2 by immunodepletion may result in the co-depletion of other factors essential for telomere end protection.

Replication defects in ΔTRF2 nuclei

When xTRF2 was immunodepleted, the overall replication efficiency of bulk DNA was significantly reduced (Fig. 4A). This reduction was recovered in ΔTRF2 nuclei treated with anti-xATR neutralizing antibody (Fig. 4C). As telomere DNAs replicate in egg extracts at relatively early time points (Supplementary text and Fig. S7 in Supporting Information), it is likely that the defectively replicated telomeres elicit ATR signals that prevent the replication of the rest of the genome at later time points (Fig. 5E, pathway c). Given that mouse TRF1 is required for the replication fork progression at telomeres (Sfeir *et al.* 2009) and that xTRF1 is absent from chromatin in interphase (Nishiyama *et al.* 2006), it is likely that xTRF2 instead of xTRF1 plays an important role in telomere replication. However, in spite of repeated trials, measurements of replicated telomeres in ΔTRF2 extracts in BrdUTP substitution experiments were unsuccessful. Further study is necessary to elucidate the mechanism underlying the defective replication of bulk and telomere DNAs in ΔTRF2 nuclei.

It is interesting that the inhibition of the general replication efficiency was restored in ΔTRF2+rTRF2 extracts, where TIFs and p-ATM were still observed (Fig. 5E, pathway b). This suggests that DNA damage responses characterized by TIFs and replication defects of bulk DNAs are caused by different downstream pathways of xTRF2 depletion. We also observed that the number of telomere FISH signals was significantly reduced in ΔTRF2 nuclei (Figs. 5A-C). DNA replication contributes to the loss of telomere FISH signals, because the loss was not observed in the geminin-treated extract. The length of telomere DNA in ΔTRF2 nuclei was similar to that in Δmock nuclei (Fig. 5D). It should be elucidated in the future how the number of telomere FISH signals is diminished in ΔTRF2 nuclei. It is also notable that the loss of telomere FISH signal is rescued by the supplementation of ΔTRF2 extracts with rTRF2, a situation

similar to the recovery of the reduced bulk DNA replication by rTRF2 and distinct to the inability of rTRF2 to suppress TIF formation. We hereby propose that two roles of xTRF2 in telomere end protection and replication: xTRF2 protects telomeres from activating DNA damage responses, probably as a member of the shelterin complex, and xTRF2 on its own regulates DNA replication (Fig. 5E).

Experimental Procedures

Antibodies, inhibitors and recombinant proteins

Anti-xTRF2 (Nishiyama *et al.* 2006), anti-xPOT1 (against the full-length polypeptide), and anti-*Xenopus* NBS1 (against the polypeptide fragment representing a.a. 392-763) rabbit antibodies were raised in our laboratory. Anti-human histone H2B rabbit antibody (#07-371) and anti-human phospho-H2AX (Ser139; γ-H2AX) rabbit antibody (#07-164) were from Upstate. Anti-human p-Rad17 (Ser645) rabbit antibody that recognizes phosphorylated *Xenopus* Rad17 (Ser650) (#03421) and anti-human p-Chk1 (Ser345) rabbit antibody that recognizes phosphorylated *Xenopus* Chk1 (Ser344) (#2348) were from Cell Signaling. Anti-human p-ATM (Ser1981) rabbit antibody that recognizes phosphorylated *Xenopus* ATM (Ser1989) was from Rockland (#600-401-398). Anti-*Xenopus* ATM rabbit antibody and anti-*Xenopus* ATR rabbit antibody were a gift from Dr. William G. Dunphy (California Institute of Technology) (Kumagai *et al.* 2004; Yoo *et al.* 2004). Anti-human Chk1 mouse antibody was from Santa Cruz (sc-8408). Anti-*Xenopus* Cds1 rabbit antibody was a gift from Dr. Takeo Kishimoto (Tokyo Institute of Technology) (Gotoh *et al.* 2001). Normal rabbit IgG was from Santa Cruz (sc-2027). Alkaline phosphatase-conjugated anti-rabbit IgG swine antibody was from DAKO (D0306). Horseradish peroxidase (HRP)-conjugated anti-rabbit IgG donkey (NA934) and HRP-conjugated anti-mouse IgG sheep antibodies (NA931) were from GE Healthcare. Alexa488-anti-rabbit IgG goat antibody was from Molecular Probes (A-11034). Caffeine was from WAKO Chemicals. KU55933 and UCN-01 were from Calbiochem. Recombinant xTRF2 was produced *in vitro* using the TNT T7Quick Coupled Transcription/Translation System (Promega). GST-tagged

Xenopus geminin was produced in *E. coli* (Kumagai *et al.* 2004) and purified using glutathione-Sepharose high-performance beads (GE Healthcare).

Xenopus extracts and immunodepletion

Xenopus interphase extracts were prepared as described (Blow 1993). Demembraned *Xenopus* sperm chromatin was incubated with *Xenopus* egg extracts at 23˚C. For the immunodepletion of xTRF2, 100 µl of interphase extract was treated three times with 30 µ l of 50% Protein A-Sepharose 4 Fast Flow beads solution (GE Healthcare) conjugated with 30 µg of anti-xTRF2 antibody. For control (mock-depleted) extracts, 30 µg of normal rabbit IgG, instead of anti-xTRF2, was similarly used. To supplement rTRF2, reticulocyte lysate producing rTRF2 or its control was directly added to the *Xenopus* extracts. Geminin was added to the extracts to a final concentration of 30 µg/ml to inhibit replication. The final concentrations of the other inhibitors in extracts were as follows: 10 µM KU55933, 5 ng/µl anti-xATR antibody, 100 nM UCN-01, and 3 mM caffeine. Reconstitution of nuclei in extracts was performed as described (Blow 1993). Chromatin fractions and nuclear fractions were prepared as described (Yoo *et al.* 2006). *Xenopus* CSF-arrested extracts were prepared according to Murray (Murray 1991) with minor modifications (Nishiyama *et al.* 2000).

Indirect immunofluorescence and FISH analyses of _Xenopus_ nuclei

Indirect immunofluorescence and FISH analyses were performed as described (Funabiki & Murray 2000; Nabetani *et al.* 2004). Demembraned sperm chromatin (500-2,000 nuclei per µl) was incubated with 20 µl of extracts for 90 min. The reaction was terminated by the addition of 80 µ l of chromosome dilution buffer (10 mM

HEPES-KOH pH7.4, 200 mM KCl, 0.5 mM $MgCl_2$, 0.5 mM EGTA, and 250 mM sucrose) and incubation for 15 min at room temperature. Samples were fixed for 5 min with 300 µl of chromosome fixation buffer (20% glycerol, 0.5% Triton X-100, and 3.7% formaldehyde in MMR buffer; MMR buffer contains 100 mM NaCl, 2 mM KCl, 5 mM HEPES-KOH, pH 7.5, 1 mM $MgCl_2$, 2 mM $CaCl_2$, and 0.1 mM EGTA) and chromatin was attached onto poly-L-lysine-coated cover slips by centrifugation through a 5 ml cushion of 40% glycerol in MMR buffer at 1,580 xg, 30 min. After the samples were washed twice with PBS, nuclei were fixed onto cover slips with ice-cold methanol for 10 min. The fixed nuclei were permeabilized by treatment for 10 min at room temperature with 0.5% Triton X-100 in PBS. Samples were washed with PBS three times and treated with the blocking buffer (3% bovine serum albumin and 0.2% Triton X-100 in PBS for xTRF2, p-Rad17, and xNBS1; 0.1% bovine serum albumin, 0.1% skim milk and 0.2% Triton X-100 in PBS for γ-H2AX) for 15 hr at 4˚C. Samples were incubated with primary antibodies diluted with 100 µl of the blocking buffer, overlaid by a cover slip and incubated for 15 hr at 4˚C. After washing three times with PBS, the samples were treated with secondary antibodies in the blocking buffer for 2 hr at room temperature. The samples for FISH experiments were prepared as described (Nabetani *et al.* 2004). The samples were counterstained for DNA with 1 µg/ml DAPI in PBS. Fluorescent images were obtained with a DeltaVision microscope (Applied Precision) equipped with a charge-coupled device camera (Photometrics). Images were processed with softWoRx (Applied Precision) using the same signal strength scale in all experiments and Photoshop (Adobe) software.

In gel hybridization

The preparation of genomic DNA was performed as described (Cohen *et al.* 1999) with minor modifications and in gel hybridization was performed as described (Nabetani & Ishikawa 2009). Demembraned sperm chromatin was incubated with 100 µl of extracts for 90 min. The reaction was stopped by the addition of 5 volumes of 30 mM EDTA, 1% SDS, 0.5% Triton X-100, and 0.3 M NaCl, followed by incubation for 16 hr at 37˚C with 0.1 mg/ml Proteinase K. DNA was extracted with phenol treatment and phenol/chloroform treatment, digested with 0.2 mg/ml RNase A for 6 hr at 37˚C, and precipitated with isopropanol. DNA was digested with *Hae*III for 16 hr at 37˚C and precipitated with ethanol.

Replication assay

Replication of sperm nuclei was performed as described (Dasso & Newport 1990; Walter *et al.* 1998) with minor modifications. Briefly, 40 µl of the *Xenopus* egg extracts including 500 nuclei/µl of sperm chromatin was incubated in the presence of 0.2 µCi (3000 Ci/mmol) of [α-^{32}P]dCTP. Two µl aliquots were dispensed at 15 min intervals and the reactions were terminated by mixing with 18 µl of stop solution (5 mM Tris-HCl, pH 8.0, 1% SDS, 5 mM EDTA, and 0.6 mg/ml proteinase K). The samples were subjected to agarose gel electrophoresis and autoradiographs were analyzed and quantitated with a Typhoon 9400 phosphorimager and ImageQuant software (GE Healthcare). Replication efficiency was determined as described previously (Blow & Laskey 1986), where the endogenous concentration of dCTP in the extracts was assumed to be 50 µM.

Acknowledgments

We are grateful to Dr. T. Kishimoto (Tokyo Institute of Technology) for anti-*Xenopus* Cds1 antibody, Dr. W. G. Dunphy (California Institute of Technology) for anti-*Xenopus* ATR antibody and anti-*Xenopus* ATM antibody, Dr. J. Shampay (Reed College) for pOS1 plasmid, and Dr. H. Takisawa (Osaka University) for the *Xenopus* geminin gene. We appreciate the helpful advices of Dr. J. C. Walter (Harvard Medical School) on *Xenopus* experiments. We also thank Ms. M. Tamura for technical assistance and Ms. A. Katayama, M. Sakamoto, M. Sasaki, K. Fujimaki, and F. Maekawa for excellent secretarial work. This work was supported by a Grant-in-Aid for Cancer Research from the Ministry of Education, Culture, Sports, Science and Technology, Japan (to F.I.).

References

Abraham, R.T. (2001) Cell cycle checkpoint signaling through the ATM and ATR kinases. *Genes Dev* **15**, 2177-2196.

Bakkenist, C.J., Drissi, R., Wu, J., Kastan, M.B. & Dome, J.S. (2004) Disappearance of the telomere dysfunction-induced stress response in fully senescent cells. *Cancer Res* **64**, 3748-3752.

Blow, J.J. (1993) Preventing re-replication of DNA in a single cell cycle: evidence for a replication licensing factor. *J Cell Biol* **122**, 993-1002.

Blow, J.J. & Laskey, R.A. (1986) Initiation of DNA replication in nuclei and purified DNA by a cell-free extract of Xenopus eggs. *Cell* **47**, 577-587.

Chen, Y., Yang, Y., van Overbeek, M.*, et al.* (2008) A shared docking motif in TRF1 and TRF2 used for differential recruitment of telomeric proteins. *Science* **319**, 1092-1096.

Cohen, S., Menut, S. & Méchali, M. (1999) Regulated formation of extrachromosomal circular DNA molecules during development in *Xenopus laevis*. *Mol Cell Biol* **19**, 6682-6689.

Dasso, M. & Newport, J.W. (1990) Completion of DNA replication is monitored by a feedback system that controls the initiation of mitosis in vitro: studies in Xenopus. *Cell* **61**, 811-823.

De Rycker, M., Venkatesan, R.N., Wei, C. & Price, C.M. (2003) Vertebrate tankyrase domain structure and sterile α motif (SAM)-mediated multimerization. *Biochem J* **372**, 87-96.

Durkin, S.G. & Glover, T.W. (2007) Chromosome fragile sites. *Annu Rev Genet* **41**,

169-192.

Funabiki, H. & Murray, A.W. (2000) The *Xenopus* chromokinesin Xkid is essential for metaphase chromosome alignment and must be degraded to allow anaphase chromosome movement. *Cell* **102**, 411-424.

Gotoh, T., Ohsumi, K., Matsui, T., Takisawa, H. & Kishimoto, T. (2001) Inactivation of the checkpoint kinase Cds1 is dependent on cyclin B-Cdc2 kinase activation at the meiotic G_2/M-phase transition in *Xenopus* oocytes. *J Cell Sci* **114**, 3397-3406.

Karlseder, J., Broccoli, D., Dai, Y., Hardy, S. & de Lange, T. (1999) p53- and ATM-dependent apoptosis induced by telomeres lacking TRF2. *Science* **283**, 1321-1325.

Konishi, A. & de Lange, T. (2008) Cell cycle control of telomere protection and NHEJ revealed by a ts mutation in the DNA-binding domain of TRF2. *Genes Dev* **22**, 1221-1230.

Konrad, J.P., Mills, W., Easty, D.J. & Farr, C.J. (1999) Cloning and characterisation of the chicken gene encoding the telomeric protein TRF2. *Gene* **239**, 81-90.

Kumagai, A., Kim, S.M. & Dunphy, W.G. (2004) Claspin and the activated form of ATR-ATRIP collaborate in the activation of Chk1. *J Biol Chem* **279**, 49599-49608.

Lazzerini Denchi, E. & de Lange, T. (2007) Protection of telomeres through independent control of ATM and ATR by TRF2 and POT1. *Nature* **448**, 1068-1071.

Loayza, D. & de Lange, T. (2003) POT1 as a terminal transducer of TRF1 telomere length control. *Nature* **423**, 1013-1018.

McNees, C.J., Tejera, A.M., Martínez, P.*, et al.* (2010) ATR suppresses telomere fragility and recombination but is dispensable for elongation of short telomeres by

telomerase. *J Cell Biol* **188**, 639-652.

Miyoshi, T., Kanoh, J., Saito, M. & Ishikawa, F. (2008) Fission yeast Pot1-Tpp1 protects telomeres and regulates telomere length. *Science* **320**, 1341-1344.

Murray, A.W. (1991) Cell cycle extracts. *Methods Cell Biol* **36**, 581-605.

Nabetani, A. & Ishikawa, F. (2009) Unusual telomeric DNAs in human telomerase-negative immortalized cells. *Mol Cell Biol* **29**, 703-713.

Nabetani, A., Yokoyama, O. & Ishikawa, F. (2004) Localization of hRad9, hHus1, hRad1, and hRad17 and caffeine-sensitive DNA replication at the alternative lengthening of telomeres-associated promyelocytic leukemia body. *J Biol Chem* **279**, 25849-25857.

Nishiyama, A., Muraki, K., Saito, M., Ohsumi, K., Kishimoto, T. & Ishikawa, F. (2006) Cell-cycle-dependent *Xenopus* TRF1 recruitment to telomere chromatin regulated by Polo-like kinase. *EMBO J* **25**, 575-584.

Nishiyama, A., Tachibana, K., Igarashi, Y.*, et al.* (2000) A nonproteolytic function of the proteasome is required for the dissociation of Cdc2 and cyclin B at the end of M phase. *Genes Dev* **14**, 2344-2357.

Palm, W. & de Lange, T. (2008) How shelterin protects mammalian telomeres. *Annu Rev Genet* **42**, 301-334.

Sfeir, A., Kabir, S., van Overbeek, M., Celli, G.B. & de Lange, T. (2010) Loss of Rap1 induces telomere recombination in the absence of NHEJ or a DNA damage signal. *Science* **327**, 1657-1661.

Sfeir, A., Kosiyatrakul, S.T., Hockemeyer, D.*, et al.* (2009) Mammalian telomeres resemble fragile sites and require TRF1 for efficient replication. *Cell* **138**, 90-103.

Takai, H., Smogorzewska, A. & de Lange, T. (2003) DNA damage foci at dysfunctional

telomeres. *Curr Biol* **13**, 1549-1556.

van Steensel, B., Smogorzewska, A. & de Lange, T. (1998) TRF2 protects human telomeres from end-to-end fusions. *Cell* **92**, 401-413.

Walter, J., Sun, L. & Newport, J. (1998) Regulated chromosomal DNA replication in the absence of a nucleus. *Mol Cell* **1**, 519-529.

Yoo, H.Y., Jeong, S.Y. & Dunphy, W.G. (2006) Site-specific phosphorylation of a checkpoint mediator protein controls its responses to different DNA structures. *Genes Dev* **20**, 772-783.

Yoo, H.Y., Shevchenko, A. & Dunphy, W.G. (2004) Mcm2 is a direct substrate of ATM and ATR during DNA damage and DNA replication checkpoint responses. *J Biol Chem* **279**, 53353-53364.

Figure legends

Figure 1

Alignments of amino acid sequences of human and *Xenopus* TRF1 and TRF2

(A) Schematic representation of the domain structures of human and *Xenopus* TRF1s and TRF2s. Positions of acidic and basic regions, TRFH domain and Myb domain are indicated. The regions involved in the interaction with hTIN2, hApollo and the region corresponding to mTRF2 region interacting with mRap1 are indicated by bars.

(B, C) Alignments of TRF1 and TRF2 amino acid sequences of the regions required for the interactions with hTIN2, hApollo, and mRap1. Amino acid residues conserved between human and *Xenopus* TRF1s and TRF2s are hatched.

(B) Boxes represent the amino acid residues of hTRF1 involved in the interaction with hTIN2, and those of hTRF2 involved in the interaction with hApollo. Asterisks indicate amino acid residues essential for the interaction in the two interacting domains. hTRF1 D139-A-Q141 forms an anti-parallel β-sheet with hTIN2, and E146 and E192 of hTRF1 make four electrostatic interactions with hTIN2 (Chen *et al.* 2008).

(C) Boxes show the amino acid residues of hTRF2 required and sufficient for the interaction with hTIN2 (Chen *et al.* 2008), and the amino acid residues of hTRF2 corresponding to those of mTRF2 sufficient for the interaction with mRap1. Asterisks indicate amino acid residues required for mRap1-mTRF2 interaction (Sfeir *et al.* 2010).

Figure 2

Localization and immunodepletion of xTRF2 in chromatin

(A) Colocalization of xTRF2 and telomeric DNA in chromatin reconstituted in

interphase egg extracts (upper), ΔTRF2 extracts (middle) and ΔTRF2+rTRF2 extracts (bottom). Signals of indirect immunofluorescence using anti-xTRF2 antibodies (green), FISH by the telomere probe (red), and chromatins stained with DAPI (blue) are shown. Merge represents superimposed image of the three signals. Enlarged images of the area enclosed by a white square are shown on the right. Bar, 15 μm.

(B, C) Immunodepletion of xTRF2. Chromatin reconstituted in egg extracts was isolated and chromatin-bound xTRF2, xPOT1, and histone H2B (H2B, a loading control) were analyzed by immunoblotting. Results of chromatin reconstituted in ΔTRF2 or Δmock extracts are shown. (B) +rTRF2, Extracts were supplemented with rTRF2. (C) +Gem, treated with geminin. Chromatin-bound proteins derived from equal amounts of extracts were loaded and analyzed by immunoblotting experiments. In the case of the +Gem samples, DNA replication did not happen leading to the relatively weaker signals for H2B compared to the -Gem samples that duplicated chromatin by replication. Arrows indicate the position of xPOT1 signals and the fast-migrating bands are non-specific signals.

Figure 3

TIFs in ΔTRF2 nuclei

(A) Colocalization of γ-H2AX and telomere FISH foci. Examples of images of γ-H2AX (green), telomere (red) and DNA (blue) are shown. Enlarged images of the area enclosed by a white square in the merged pictures (Merge) are shown. +rTRF2, Extracts were supplemented with rTRF2. Bar, 15 μm.

(B) TIF formation was not suppressed by supplementation with rTRF2. Percentages of

γ-H2AX-positive telomere foci among all telomere foci are shown. Horizontal bars represent the averages. Extracts were supplemented with rTRF2 (+rTRF2) or buffer control (-). The number of nuclei examined was 40 in three independent experiments.

(C) TIFs were formed in a replication-independent manner. Percentages of γ-H2AX-positive telomere foci among all telomere foci are shown. Extracts were supplemented with geminin (+Gem) or buffer control (-). Horizontal bars represent the averages. The number of nuclei examined was 56 in three independent experiments.

Figure 4

Anti-xATR antibody rescues the decreased replication efficiencies of bulk DNA in ΔTRF2 nuclei

Replication efficiencies of bulk DNA in ΔTRF2 and Δmock nuclei. rTRF2 (A), an ATM inhibitor (10 μM KU55933) (B), 5 ng/μl anti-xATR neutralizing antibody (C) or a Chk1 inhibitor (100 nM UCN-01) (D) was added to the extracts as indicated.

Figure 5

Loss of telomere FISH signals in replicated chromatin in the absence of xTRF2

(A) Telomere FISH signals in ΔTRF2 nuclei. Images of telomere FISH signals (red) and DNA (blue) detected in ΔTRF2 and Δmock nuclei are presented. rTRF2 or geminin (Gem) was added to ΔTRF2 extracts prior to incubation with sperm chromatin as in Fig. 2. Bar, 15 μm.

(B, C) Number of telomere FISH signals per nucleus in rTRF2-supplemented (+rTRF2) extracts (B), geminin-treated (+Gem) extracts (C), and their buffer control (-). Horizontal bars represent the averages. The number of nuclei examined was 125 (B)

and 77 (C) each in six independent experiments.

(D) DNAs from ΔTRF2 chromatin and Δmock chromatin were digested with *Hae*III, run in a gel, and in-gel hybridized with indicated probes.

(E) Dual roles of xTRF2 in telomere replication and telomere end protection

Interphase nuclei lack xTRF1 and the shelterin complex likely consists of five proteins, xTRF2, Rap1, TIN2, TPP1, and xPOT1 (a1). Immunodepletion of xTRF2 led to the dissociation of xPOT1 from chromatin (a2). Depletion of xTRF2 activates ATM and telomere end deprotection (shown by a blue circle) (a3). xTRF2 is required for DNA replication (b1 and b2). When xTRF2 is depleted from interphase extracts (c1), the replication fork is stalled at telomeres (shown by a red circle), leading to the activation of ATR at telomeres (c2). The activated ATR represses other replication forks throughout the genome, resulting in the halting of the genome-wide replication (c3). Supplementation with rTRF2 rescued the DNA replication defects but not the deprotected telomeres, suggesting that telomere end protection requires the precise organization of the shelterin complex.

Fig. 1 Muraki *et al.*

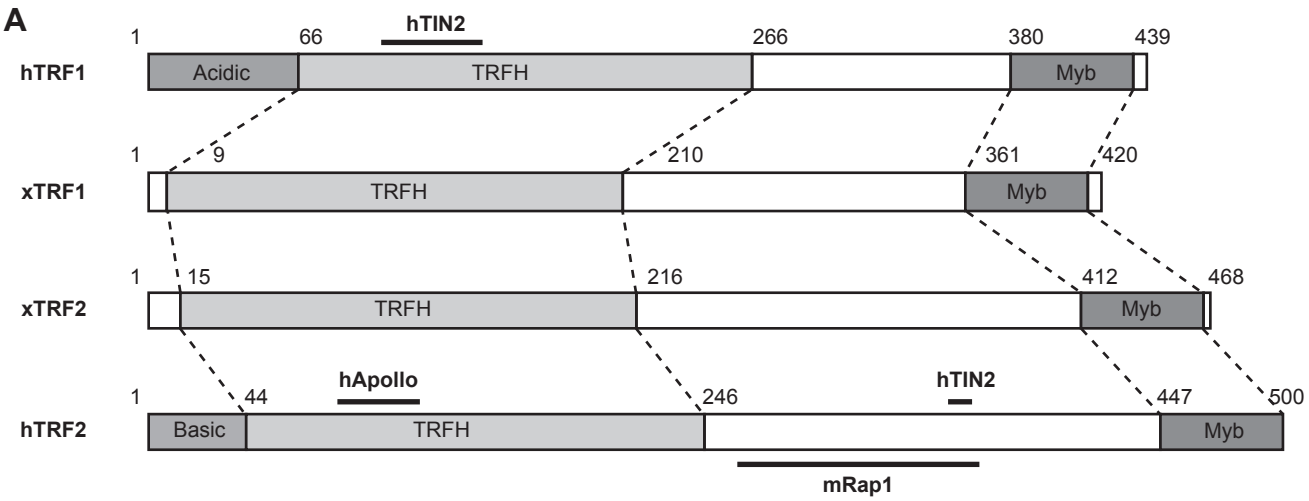

B

```
                                                  hTIN2                                                  138   142   146
                                                 102                                                     * * * * *     * 147
hTRF1   93 GRSEDFRRTRNSAEAIIHGLSSLTACQLRTIYICQFLTRIAAGKTLDAQFENDERI 148
xTRF1   36 DRTEDFQRSTHMLEWLLEGSQKLDAHR-KTIPIAQFLMRVAEGKNLDSQFDTDESL  90
xTRF2   42 DRHEDFQEIRDIVSVLLLRPLETKAQNDCKLRIMQCISRIEEGEDPDCTFNDNNNE  97
hTRF2   71 SRYGDFRQIRDIMQALLVRRLGKEHTVSRLLRVMQCLSRIEEGENLDCSFDMEAEL 126
                          83                hApollo  101 102                120
                                                                  192
                                                                  *
hTRF1  149 TPLESALMIWGSIEKEHD---KLHEEIQNLIKIQAIAVCMENGNFKEAEEVFERIF 201
xTRF1   91 TPLETALNAFNQIEEEEDLK-HLHEEIELILKVQAVVTCMEKGRFKLSAEILDRLF 145
xTRF2   98 TPLESAVGLLDIIQEEMPLDEDLFKTNKQMVKEAAVLVCIKKQKFDQAIRILKKYI 153
hTRF2  127 TPLESAINVLEMTKTEFTLTEAVVESSRKLVKEAAVIICIKNKEFEKASKILKKHM 182
```

C

```
hTRF1  275 QDKPSGNDVEMETEANLDTRKSVS------------------DKQSAVTES--SEGTVSLLRSHKN 320
xTRF1  219 QSQES-EDCEQQTNESLENKDDNSSSEYEERDVLSLSNINHVENKEDISSSDYEEAAEQLKVCNRD 283
xTRF2  225 TPTTEQEQTTLHLQNESPRSPQVVSSEADCVISYGLSVLKSKFKSLCQEEDPDTIFRGLCEMDFCR 290
hTRF2  252 STGKEDKQPAPGPVEKPPREP--ARQLRNPPTTIGMMTLKAAFKTLSGAQDSEAAFAKLDQKDLVL 315
                  260                mRap1                 291 292

hTRF1  321 LFLSKLQHGTQQQDLNKK-----ERRVG-----TPQSTKKKKESRRATESRIPVSKSQPVTPE  373
xTRF1  284 INQNELTNTTNIQETTEKSTKRHQRRLFSIAQRTPWNPDKPCTSKRLLSS-INIGKNSKENQE  345
xTRF2  291 --QDTPNDIPLEKAGTDTEESILGR----------HRKKLVVSLKQVVIDKDSQCIHLSENSN  341
hTRF2  316 PTQALPASPALKNKRPRKDENESSAPADGEGGSELQPKNKRMTISRLVLEEDSQSTEPSAGLN  378
                                  mRap1                352 hTIN2 362 366
```

Fig. 2 Muraki *et al.*

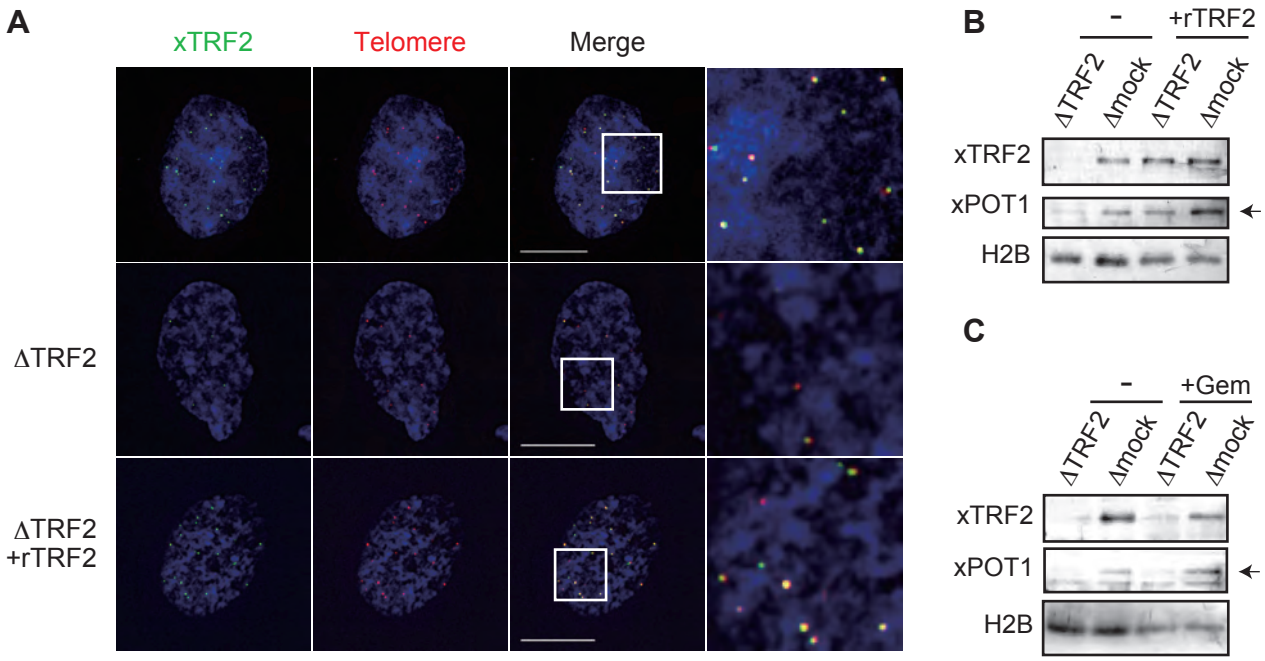

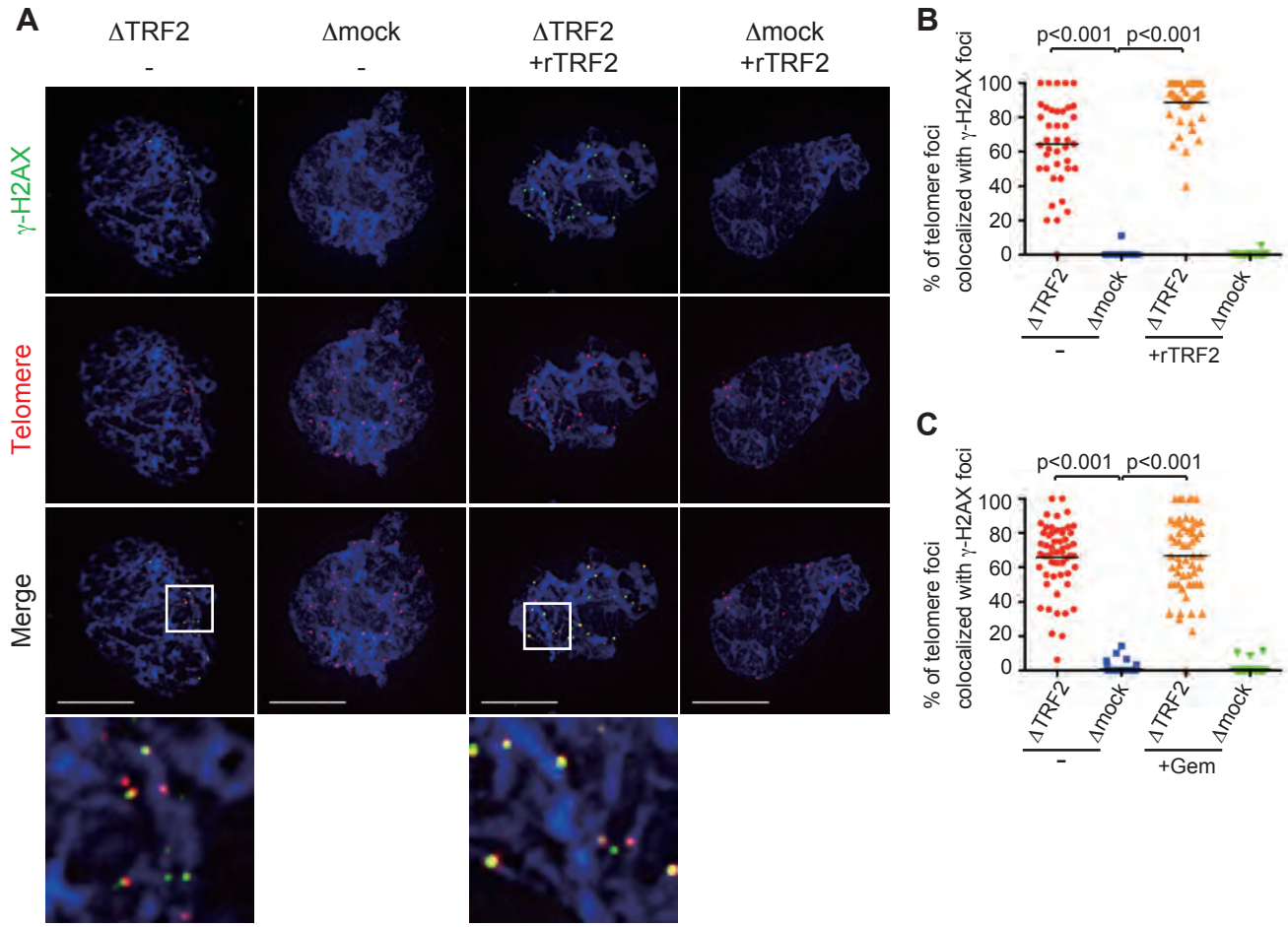

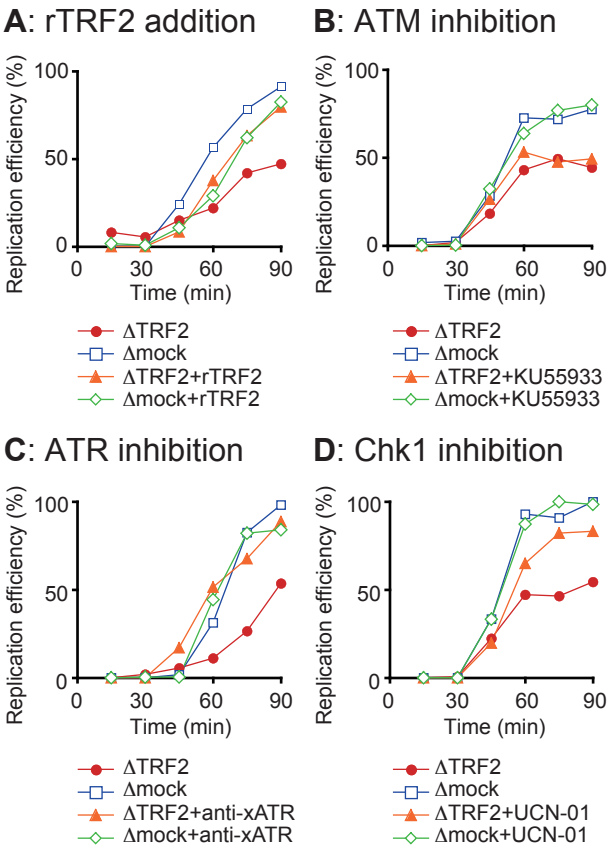

Fig. 5 Muraki *et al.*